Controller design of a robotic assistant for the transport of large and fragile objects

Julie Dumora, Julien Nicolas, Franck Geffard

Controller design of a robotic assistant for the transport of large and fragile objects

Julie Dumora[1], Julien Nicolas[1] and Franck Geffard[2]

Abstract— **This paper deals with the design of a robotic assistant for the transport of large and fragile objects. We propose a new collaborative robotic controller that fulfills the main requirements of co-transportation tasks of large and fragile objects: to execute any trajectory in a collaborative mode while minimizing the stress applied on the object by both partners in order to avoid damaging it. This controller prevents the robot from applying torques on the object while maintaining a desired orientation of the object along the transport trajectory in order to follow the operator. An original feature of our approach is to care about torques applied by both partners (not only by operator) during any co-manipulation trajectory execution. It leads to a novel outcome: the minimization of stress applied by both partners on a large and fragile object during its transport on any trajectory. We demonstrate the effectiveness of this approach in a collaborative transportation task.**

I. INTRODUCTION

This work focuses on human-robot joint collaboration for achieving large and fragile object transportation tasks. Such tasks are extensively performed in industrial contexts, for example in aerospace industry as well as in construction field. Our work has been driven by an industrial use-case of the European MERGING project: the manufacture of composite parts for the automotive sector. The manufacturing process of composite parts requires the transport of large and fragile parts like foam blocks into a mould where they are then precisely positioned.

The characteristics (large and fragile) of the transported objects lead to involve several people for executing the task and often cause ergonomics issues. Industrial assisting systems are sometimes used but suffer from a lack of flexibility. In this regard, large and fragile object co-manipulation has resulted in many research and development efforts in the field of robotics and in particular in the human-robot joint collaboration domain.

A necessary requirement for a successful physical human-robot interaction is that the robot easily moves when an external force is applied on it. This feature, which is called the robot backdrivability, is obtained by mechanical properties of actuators [1] or by an impedance control [2][3]. However, a direct consequence of the behavior of a backdrivable robot in jointly human-robot manipulation of a large object is an ambiguity on the interpretation of the operator's force: does the operator want to rotate or to translate the object (Fig. 1)? The operator can tackle this problem himself by simultaneously applying a torque and a force at his gripping point in order to perform a lateral translation (Fig. 1)[4].

[1] CEA Tech Nouvelle Aquitaine, Interactive Robotics Plateform, Pessac, France firstname.lastname@cea.fr

[2] Université Paris-Saclay, CEA, List, F-91120, Palaiseau, France franck.geffard@cea.fr

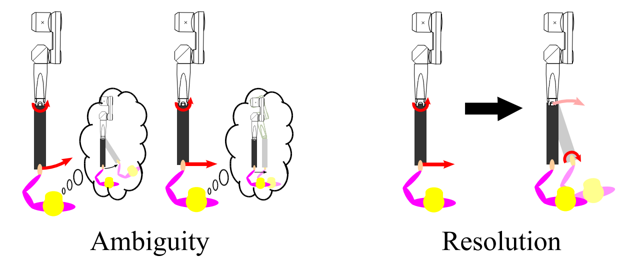

Fig. 1. Ambiguity at the backdrivable robot gripping point between an intention of rotation and an intention of translation and its resolution by the operator.

Considering a large object of length l with a negligible weight carried out jointly by a human at one side O and a robot at the opposite side A (Fig. 2), the moment of inertia J_{O_z}, which quantifies the resistance of the system to be rotated from operator gripping point O, is equal to:

$$J_{O_z} = m^* l^2 \tag{1}$$

Equation (1) means that the apparent inertia m^* of the backdrivable robot, which cannot be reduced [5], is amplified by the square of the distance between the partner's gripping points. The torque applied by the operator to move the object side grasped by the robot is as important as the robot inertia and the object length are higher. For these reasons, a back-drivable robotic partner for human-robot shared manipulation lost the painless assistance interest, as it requires the operator to provide more effort in order to fight against its inertia.

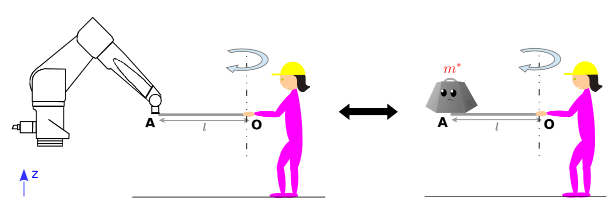

Fig. 2. Problem statement.

In this regard, the main challenge tackled in this paper is to enable simultaneous motions of the operator and the robot gripping points without damaging the large and fragile object and by preserving the operator from applying high efforts.

We contend that collaborative transport tasks of a large and fragile object can be made more reliable by having both partners that apply only forces (no torques) as human-human dyad usually does. To this end, we have designed a new robotic controller leading to an active follower robotic assistant: the robot actively moves on the transport trajectory according to the displacement of the operator. Moreover, this controller design prevents the robot from the ability to apply torques.

After discussing related work in the following section, we will present our controller design of a robotic assistant for the transport of large and fragile objects in Section III. In Section IV, we will present experimental results demonstrating the advantages of our active follower robotic assistant design. Finally, we will draw some conclusions and outline future work in Section V.

II. RELATED WORK

Several strategies, which aim at easing the simultaneous motions of the human and the robot gripping points, have been published in the last decades.

One of the first method, which has emerged in the literature, is to impose non-holonomic constraints to the robot [6][7][8]. Thereby, the robot allows only certain displacements. This solution compels the operator to combine a series of motions in order to perform one single prohibited movement of the object. A study presented in [7] shows that keeping movement redundancies is more effective to promptly fulfill a complex task. Moreover, allowing holonomic displacements ensures a sufficient condition, if at least one path exists, to reach a target even in a narrow environment [9]. This condition is not assured by non honolomic methods that can only prove the controllability of the system [8]. In a previous work [10], we endow the robot with a library of assistances for performing standard collaborative motions ensuring movement redundancies. According to the haptic cues naturally transmitted by the human partner, the robot selects in real-time the suitable assistance for the current intended collaborative motion. The library of assistances involves constraining different degrees of freedom of a backdrivable robot in order to prevent the operator from applying high torques. For example, for laterally translating an object, the robot control prevents from a rotation at the robot gripping point. In that case, the robot counteracts the intended rotation by applying a torque at its gripping point. As backdrivable robots have a non-negligible apparent inertia, we can apply the Varignon's formula:

$$\mathbf{M}_A = \mathbf{M}_O + \mathbf{AO} \times \mathbf{F} \tag{2}$$

with $\mathbf{M}_A \in \mathbb{R}^3$ the torques applied in A, $\mathbf{M}_O \in \mathbb{R}^3$ the torques applied in O, $\mathbf{AO} \in \mathbb{R}^3$ the position vector between both gripping point and $\mathbf{F} \in \mathbb{R}^3$ the force applied by the operator who intends to move the object. According to (2), the torque applied at the robot gripping point $\mathbf{M}_A$ increases with the distance between the operator and the robot gripping points and with the force applied by the operator $\mathbf{F}$ who intends to laterally translate the object. Although this work has proved its efficiency for large objects co-manipulation, it is not suited to co-manipulate large and fragile objects because of the risk of damaging the fragile object that increases with the length of the object. The same issue is met in [11] that proposes to constrain the robot on a desired trajectory.

In light of those assessments, in order to successfully and smoothly carry out a joint collaborative task involving a fragile and large object, a robotic partner should not only permit holonomic movement of the object but also actively participate to its motion in order to preserve the operator and the robot from applying constraints on the co-manipulated object.

Under the assumption that the task is known and quite repetitive, the most common approach is to design a proactive robotic partner. This means that the robot anticipates human actions thanks to its task knowledge and actively participates to the effort sharing. The most common framework is to use programming-by-demonstration. The aim is to learn the task model to reproduce it [12][13]. Each of these strategies has been compared with a backdrivable robot without any assistance. Experimental studies [14][15] highlighted the ability of proactive robots to reduce human operator effort. However, a psychology study in [14] showed that human operators feel more comfortable and safe with a passive robot. This result can be interpreted by the difficulty of the human to predict the behavior of a robot that continuously learns during tasks, or that has to estimate parameters for its trajectory generation.

Under the assumption that the task is only partially known and to face unexpected events or obstacles, another strategy consists in feedback motion planning [9]. However, the proposed method requires object inverse dynamics in order to calculate wrench to apply on the object according to the planned trajectory. This information is difficult to obtain for each object in an industrial context.

Another interesting strategy consists in compensating the angle of the robot end-effector in order to control the translation velocity [16][17] or the force [18][19] of the robot. However, these works are limited to the assistance of straight line motions. Therefore, they are well suited for lifting an object but not for transporting it or for precisely positioning it. In order to allow rotations around the operator gripping point, the authors in [6] combine this angle approach with a force control mode realized with a force/torque sensor at the operator gripping point. However, this strategy encounters the well-known stability issue due to the non-colocalisation of measures [20][21]. Hence, poor co-manipulation performance might be obtained, which is not appropriate for performing large and fragile object co-manipulation tasks. Authors in [22] use visual information in order to maintain a table horizontally while transporting it. Displacements in the horizontal plane are performed with a reactive pattern generator presented in [23]. In this work, the operator has to apply torques in order to give his intention of primitive motions involving lateral displacements of the robot.

Our paper goes beyond the state-of-the-art by extending the angle approach at any kind of trajectory. This work expands also the approach of [11] in order to jointly transport large and fragile objects without applying heavy stress on the object. Our controller design tackles the issues encountered in the state-of-the-art approaches described above in order to efficiently transport a large and fragile object:

- Any kind of motions and not only straight lines can be performed.
- No torques have to be applied at the operator and the robot gripping points.
- Ergonomy enhancement: inhibition of the robot apparent inertia feeling at the operator gripping point.
- No extra sensors are needed at the operator gripping point.
- An easy predictability of the robot behavior is ensured for the human partner.

III. ASSISTIVE ROBOTIC CONTROLLER FOR LARGE OBJECT TRANSPORT

A. Concept

The strategy consists in designing an active follower robotic partner:

- The human operator is the leader of the dyad in order to handle the displacement of the object along the transport trajectory.
- The robot is the follower in order to avoid heavy stress on the fragile object due to a plan disagreement.
- The robot actively handles its gripping point displacement in order to prevent the operator from applying high torques.

To that end, we propose to:

- Allow rotations at the robot gripping point with a zero-force mode that prevent from robot torques application.
- Correct the object orientation, that corresponds to an angle α at the robot gripping point by a displacement of the robot gripping point along the transport trajectory (Fig. 3).

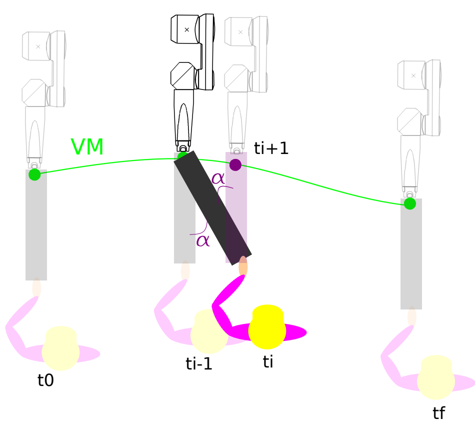

Fig. 3. Controller principle.

The partial knowledge of the task plan is necessary to apply our approach. At least the target point has to be known. This condition can easily be fulfilled in an industrial context, for instance, with vision or with programming-by-demonstration.

B. Control law of the system

Notation: Vectors and matrices are noted in bold. $\mathbf{X} = \{\mathbf{X}_{trans} \in \mathbb{R}^3, \mathbf{X}_{rot} \in G\} \in \mathbb{R}^3 \times G$ is a vector representing a displacement or a Cartesian position of a mechanism, with G the quaternion Group and $\mathbf{X}_{rot}$ a unit quaternion.
$\mathbf{W}_P = \{\mathbf{F} \in \mathbb{R}^3, \mathbf{M}_P \in \mathbb{R}^3\} \in \mathbb{R}^6$ is the wrench applied in P with $\mathbf{F}$ the force components and $\mathbf{M}_P$ the torques applied in P.
$\mathbf{q} = \{q_0, \ldots, q_N\} \in \mathbb{R}^N$ is a vector representing the joint positions of a N-joints mechanism.
$\dot{\mathbf{q}} \in \mathbb{R}^N$ is a vector representing the joint velocities of a N-joints mechanism.
$\boldsymbol{\tau} \in \mathbb{R}^N$ is a vector representing the joint torques applied on a N-joints mechanism.
$\mathbf{J}_P \in \mathbb{R}^{6 \times N}$ is a matrix representing the Jacobian of a N-joints mechanism reduced in P.

The overall system architecture consists of two main components (Fig. 4): a transport trajectory following component and an operator following component.

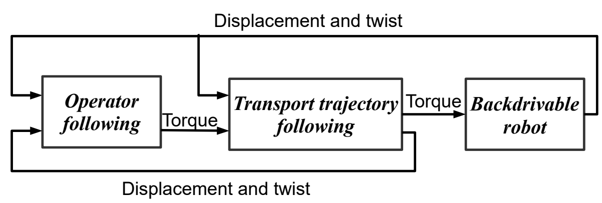

Fig. 4. Block diagram of the system architecture.

Transport trajectory following component

The transport trajectory following component contains the parametrization of the trajectory and the control law to execute this trajectory in a collaborative mode.

The transport trajectory following in a shared mode is carried out with a virtual motion guide. The guide is implemented according to the virtual mechanism (VM) concept [24]. The displacement of the robot end-effector $\mathbf{X}$ and the displacement of the virtual mechanism $\mathbf{X}_{vm}$ are coupled by a spring-damper system ($\mathbf{K} \in \mathbb{R}^{6\times6}$, $\mathbf{B} \in \mathbb{R}^{6\times6}$) (Fig. 5). Thus, the robot end-effector can be moved easily along the degrees of freedom of the virtual mechanism, *i.e.* the constraining path, but not away from it.

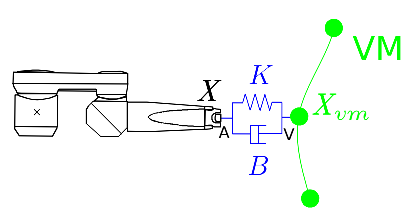

Fig. 5. Virtual Mechanism concept.

The equation of this coupling is:

$$\mathbf{W}_A = \mathbf{K}(\mathbf{X}_{vm} - \mathbf{X}) + \mathbf{B}(\dot{\mathbf{X}}_{vm} - \dot{\mathbf{X}}) \quad (3)$$

with $\mathbf{W}_A$ the wrench applied by the mechanical link at the robot end-effector A.

We assume that the VM has the dynamics of a damper. The equation of its dynamics in the joint space is:

$$\boldsymbol{\tau}_{vm} = \mathbf{B}_{vm}\dot{\mathbf{q}}_{vm} \tag{4}$$

with $\boldsymbol{\tau}_{vm} \in \mathbb{R}^N$ the torque applied on each joint of the VM, $\dot{\mathbf{q}}_{vm}$ the joint velocity of the VM and $\mathbf{B}_{vm} \in \mathbb{R}^{N\times N}$ the diagonal matrix filled with the damping parameter of each joint and where N represents the number of joints of the VM.

To fulfill the condition of mechanical balance, the sum of wrenches applied on the spring-damper link is null:

$$-\mathbf{W}_A - \mathbf{W}_V = 0 \tag{5}$$

with $\mathbf{W}_V$ the wrench applied by the mechanical link at the VM end-effector V.

$\mathbf{J}_V$ is the Jacobian matrix of the VM such as:

$$\dot{\mathbf{X}}_{vm} = \mathbf{J}_V\dot{\mathbf{q}}_{vm} \tag{6}$$

According to (3), (4), (5) and (6), we obtain:

$$\dot{\mathbf{q}}_{vm} = (\mathbf{B}_{vm} + \mathbf{J}_V^T\mathbf{B}\mathbf{J}_V)^{-1}(-\mathbf{J}_V^T(\mathbf{K}(\mathbf{X}_{vm} - \mathbf{X}) - \mathbf{B}\dot{\mathbf{X}})) \tag{7}$$

The block diagram of the control law of this component is reminded in the box "Transport trajectory following" of Fig. 6.

The translation components of the geometric model L_{vm} of the virtual mechanism define the constraining path. Two critical conditions to define this constraining path are to (i) pass through the defined waypoints and (ii) the first derivatives are continuous at the defined waypoints in order to be compatible with virtual mechanism framework (use of Jacobian $\mathbf{J}_V$). This constraining path is defined with multi-dimensional Akima splines (MDSplines) [11] that fulfill the above-mentioned conditions. Moreover, this framework uses only the values from neighboring waypoints in the construction of the coefficients of the polynomial interpolation. It means no large system of equations has to be solved, which is essential to compute L_{vm} in the real-time controller at each timestep.

In order to prevent the robot from applying torques, the rotation components of the geometric model L_{vm} of the VM are defined by a spherical joint.

Finally, the geometric model L_{vm} of the VM is defined by:

$$\mathbf{X}_{vm} = L_{vm}(\mathbf{q}_{vm}) = \begin{bmatrix} MDSpline_x(q_{vm,0}) \\ MDSpline_y(q_{vm,0}) \\ MDSpline_z(q_{vm,0}) \\ q_{vm,1} \\ q_{vm,2} \\ q_{vm,3} \\ q_{vm,4} \end{bmatrix} \tag{8}$$

with $\mathbf{q}_{vm} \in \mathbb{R}^5$ the joint position of the virtual mechanism, that has 5 degrees of freedom: $q_{vm,0}$ the path-length curvilinear parameterization of MDSplines and $q_{vm,1}$ to $q_{vm,4}$ the quaternion components defining the position of the VM in the spherical joint.

The Jacobian of the VM $\mathbf{J}_V \in \mathbb{R}^{6\times 5}$ is equal to:

$$\mathbf{J}_V = \frac{\partial L_{vm}(\mathbf{q}_{vm})}{\partial \mathbf{q}_{vm}} =$$

$$\begin{bmatrix} M\dot{D}Spline_x(q_{vm,0}) & 0 & 0 & 0 & 0 \\ M\dot{D}Spline_y(q_{vm,0}) & 0 & 0 & 0 & 0 \\ M\dot{D}Spline_z(q_{vm,0}) & 0 & 0 & 0 & 0 \\ 0 & -2q_{vm,2} & 2q_{vm,1} & -2q_{vm,4} & 2q_{vm,3} \\ 0 & -2q_{vm,3} & 2q_{vm,4} & 2q_{vm,1} & -2q_{vm,2} \\ 0 & -2q_{vm,4} & -2q_{vm,3} & 2q_{vm,2} & 2q_{vm,1} \end{bmatrix}$$

The inferior submatrix represents the relationship between the angular velocity and the derivative quaternion.

Operator following component

The operator following component contains the control law to generate a displacement of the virtual mechanism (and thus of the robot end-effector attached to the VM) according to the robot's wrist angle.

The robot end-effector position $\mathbf{X}$ is linked to the desired object position $\mathbf{X}_d$ with a spring-damper system ($\mathbf{K}_\alpha \in \mathbb{R}^{6\times 6}$, $\mathbf{B}_\alpha \in \mathbb{R}^{6\times 6}$):

$$\mathbf{W}_{\alpha,A} = \mathbf{K}_\alpha(X_d - X) + \mathbf{B}_\alpha(\dot{\mathbf{X}}_d - \dot{\mathbf{X}}) \tag{9}$$

with $\mathbf{W}_{\alpha,A}$ the wrench applied by the coupling link at the end-effector of the robot A.

As we want to maintain the object orientation by moving the position of the robot end-effector that is already virtually linked to the VM (see Compliant coupling box on Fig. 6), the translation components of the coupling gains $\mathbf{K}_\alpha$ and $\mathbf{B}_\alpha$ are set to zero. In the remainder of this section, we will explain the exploitation of the rotation components.

From Varignon's formula (2), we can deduce the wrench $\mathbf{W}_O$ applied at the operator gripping point O:

$$\mathbf{W}_O = \begin{bmatrix} \mathbf{I}_{3x3} & \mathbf{0}_{3x3} \\ \mathbf{AO}^\times & \mathbf{I}_{3x3} \end{bmatrix}^{-1} \mathbf{W}_{\alpha,A} \tag{10}$$

with

$$\mathbf{AO}^\times = \begin{bmatrix} 0 & -AO_2 & AO_1 \\ AO_2 & 0 & -AO_0 \\ -AO_1 & AO_0 & 0 \end{bmatrix} \tag{11}$$

The force components $\mathbf{F}$ of the wrench $\mathbf{W}_O$ correspond to the reactive forces that the operator would intend to apply virtually on the robot to maintain the desired orientation (Fig. 7). As we want to move the robot gripping point along the virtual mechanism in order to maintain the desired orientation, this intended reactive force is applied on the VM, as $\mathbf{F}_\alpha$ (Fig. 7):

$$\mathbf{F}_\alpha = -\mathbf{F} \tag{12}$$

$\mathbf{F}_\alpha$ is then projected in the spline frame $\mathscr{F}_\mathrm{S}$ (Fig. 8):

$$^{\mathrm{S}}\mathbf{F}_\alpha = {}^{\mathrm{S}}\mathbf{R}\mathbf{F}_\alpha \tag{13}$$

with $^{\mathrm{S}}\mathbf{R}$ the rotation matrix from the robot base frame into the spline frame. $\mathscr{F}_\mathrm{S}$ is calculated at each cycle time. The Y-axis corresponds to the tangent of the spline, and is oriented

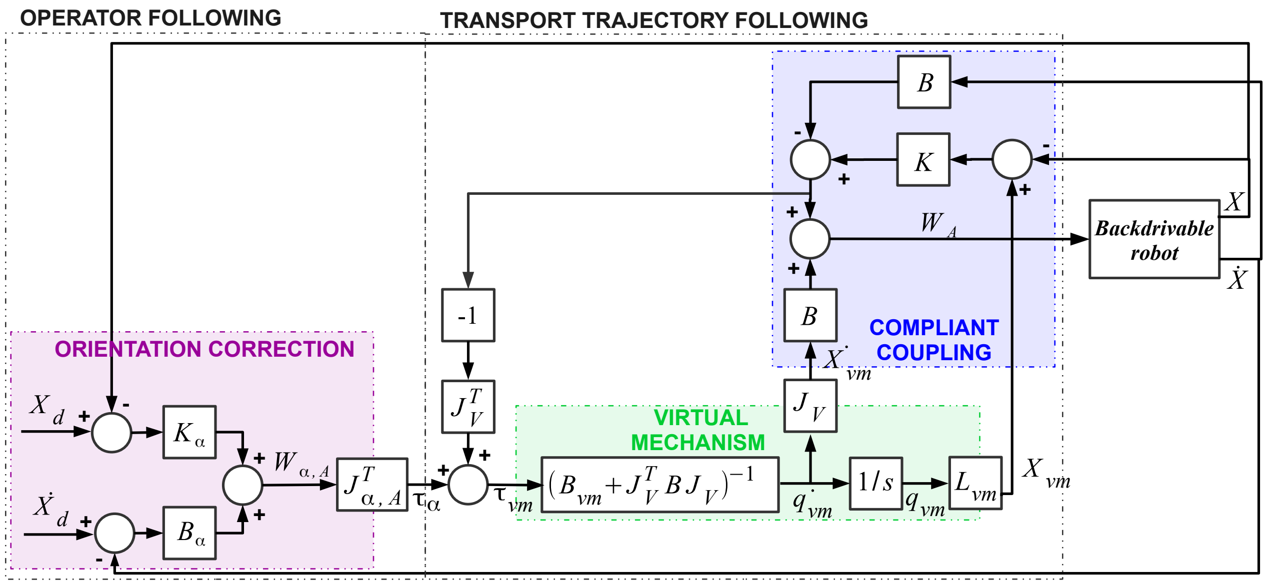

Fig. 6. Block diagram of the control system.

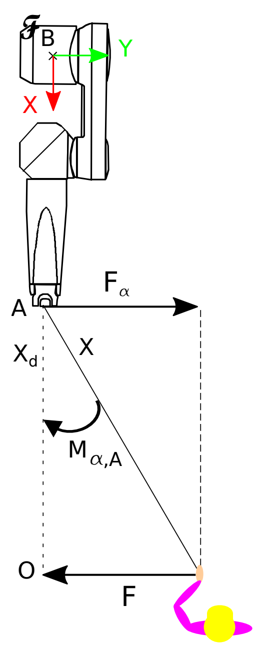

Fig. 7. Illustration of $\mathbf{F}_\alpha$ forces generated according to the coupling between the robot and the desired orientation. For clarity's sake, the example is presented in the plane (X,Y).

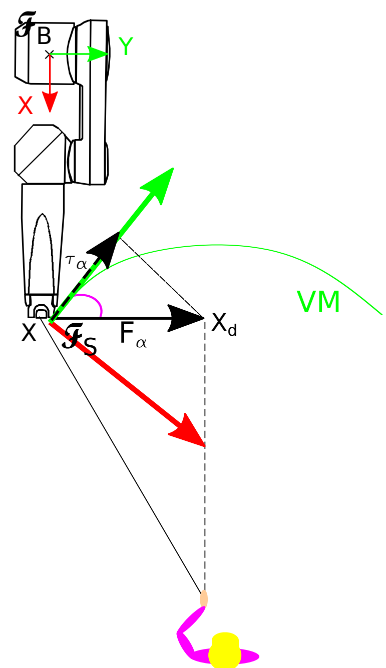

Fig. 8. Illustration of the projection of the force $\mathbf{F}_\alpha$ in the joint virtual mechanism space. For clarity's sake, the example is presented in the plane (X,Y).

along the positive direction of the spline, which is dependent on the order of waypoints definition. We project ${}^{S}\mathbf{F}_\alpha$ in the joint space of the virtual mechanism in order to obtain the torque $\boldsymbol{\tau}_\alpha$ required to move the VM (Fig. 8). It leads to the following equation:

$$\boldsymbol{\tau}_\alpha = ({}^{S}\mathbf{J}^T_{\alpha,V})\,{}^{S}\mathbf{W}_{\alpha,V} \tag{14}$$

with ${}^{S}\mathbf{W}_{\alpha,V} \triangleq \begin{bmatrix} {}^{S}\mathbf{F}_\alpha & \mathbf{0}_{3,1} \end{bmatrix}^T$ and the Jacobian ${}^{S}\mathbf{J}_{\alpha,V} \in \mathbb{R}^{6\times 5}$, which is reduced at the VM end-effector V in the spline frame, is defined by:

$${}^{S}\mathbf{J}_{\alpha,V} = \begin{bmatrix} 0 & 0 & 0 & 0 & 0 \\ 1 & 0 & 0 & 0 & 0 \\ 1 & 0 & 0 & 0 & 0 \\ 0 & 0 & 0 & 0 & 0 \\ 0 & 0 & 0 & 0 & 0 \\ 0 & 0 & 0 & 0 & 0 \end{bmatrix} \tag{15}$$

We want to project ${}^{S}\mathbf{F}_{\alpha}$ in the joint space of the virtual mechanism, the three last lines of ${}^{S}\mathbf{J}_{\alpha,V}$ are therefore set to zero. Moreover, the torque obtained by the projection is used to move the VM along the spline, *i.e.* to obtain $q_{vm,0}$, thus only the first column is relevant, the others are therefore set to zero. The first component of the first column of ${}^{S}\mathbf{J}_{\alpha,V}$ is null because the force in the direction through both gripping points does not generate a rotation of the robot's wrist. The two other directions of the force resulting in a rotation of the robot's wrist, the corresponding components therefore participate to move the VM and thus are projected in the joint space of the VM.

From (10), (11), (12), (13), (14), (15), we obtain:

$$\boldsymbol{\tau}_{\alpha} = \mathbf{J}_{\alpha,A}^{T}\mathbf{W}_{A} \tag{16}$$

with $\mathbf{J}_{\alpha,A}$ the Jacobian reduced at the robot end-effector A in the spline frame:

$$\mathbf{J}_{\alpha,A}^{T} = {}^{S}\mathbf{J}_{\alpha,V}^{T} \begin{bmatrix} {}^{S}\mathbf{R} & \mathbf{0}_{3,3} \\ \mathbf{0}_{3,3} & {}^{S}\mathbf{R} \end{bmatrix} \begin{bmatrix} -\mathbf{I}_{3,3} & \mathbf{0}_{3,3} \\ \mathbf{0}_{3,3} & \mathbf{0}_{3,3} \end{bmatrix} \begin{bmatrix} \mathbf{I}_{3x3} & \mathbf{0}_{3x3} \\ \mathbf{AO}^{\times} & \mathbf{I}_{3x3} \end{bmatrix}^{-1}$$

The torque $\boldsymbol{\tau}_{\alpha}$ is added to the torque generated by the coupling between the virtual mechanism and the robot in order to move the virtual mechanism along the defined trajectory.

The block diagram of the control system is presented Fig. 6. This version of the control law is in the Spatial frame (or fixed frame) corresponding for us to the robot base frame or to the environnement frame. In this version, the desired orientation $\mathbf{X}_{d}$ is not compelled to follow the curve orientation of the virtual spline. However, this control law can also be used for the Body frame (or moving frame) version by transforming $\mathbf{X}_{d}$ in the Body frame into the base Spatial frame (as we did in the experimental evaluation section). Note that the conventional Body frame (or moving frame) version of this control law may also be derived by applying the projection (13) before the controller $\mathbf{K}_{\alpha}/\mathbf{B}_{\alpha}$. In this latest version, the operator then needs to follow the curve orientation of the spline.

IV. EXPERIMENTAL CONFRONTATION

In order to highlight the benefits of our extension of [25] to co-transport large and fragile objects, the objective is to compare both methods on a joint collaborative transport task. Both of these methods enable to assist the path following with a given orientation along the path. The work in [25] proposes a passive assistant corresponding to a backdrivable robot coupled with a virtual mechanism described with the XSpline framework. In the following section, our approach is called *active assistant* and the method proposed in [25] is called *passive assistant*.

A. Experimental setup

We carried out the experiment on a 4-DOF articulated arm manipulator (Fig. 9). However, it is important to notice that the controller presented in the previous section is working for co-transport tasks in 6-DOF. The choice of the robot has been made only according to the availability of the arm manipulator in the lab. This manipulator is mechanically backdrivable. Otherwise, it is necessary to implement an admittance control at the lower level. The transported object is a bar of 1.8 meters long. The end-effector of the robot is rigidly attached to one end of the bar while an operator's handle is fixed on the other end. In order to estimate the stress applied on the object, we chose a rigid bar and observe the wrench at each extremity. To that end, one 6-axis Force/Torque sensor has been mounted between the wrist of the robot and the bar and another 6-axis Force/Torque sensor has been mounted between the bar and the operator's handle. Wrenches were recorded at 1kHz.

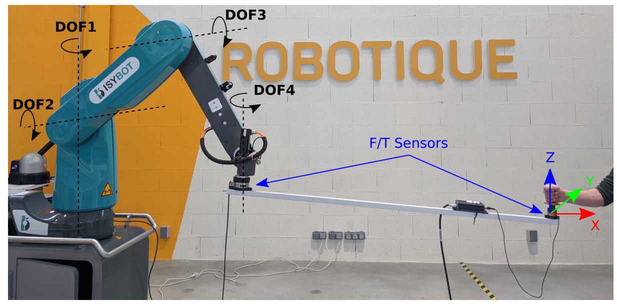

Fig. 9. Experimental setup.

The same stiffness and damping gains $\mathbf{K}$ and $\mathbf{B}$ of the robot-VM coupling have been used for both methods because they are independent of the defined VM. They have been set empirically as well as the stiffness and damping gains $\mathbf{K}_{\alpha}$ and $\mathbf{B}_{\alpha}$ applied for the wrist's angle correction. The dynamics of the VM $\mathbf{B}_{vm}$ has also been empirically tuned such that the operator does not feel a resistance of the VM in the authorized directions. The same tuning has been used for both methods.

The experimental confrontation was performed by a participant who did not contribute to the development of either of the two methods. The participant was trained to perform different transport tasks with both methods before recording the data. The participant taught four waypoints by demonstration (Fig. 10) in order to define the transport task. The desired orientation was computed in order to keep the object orientation orthogonal to the constraining path (Fig. 10). Between points, we used a spherical cubic interpolation of quaternions (SQUADs) [25]. The same trajectory was used for the transport task execution with both methods. The operator executed the defined transport task for the first time with the active assistance, then with the passive assistance.

B. Results and discussion

With a 4-DOF robotics arm, the controller is active only on given directions. For this reason, we present only the components of wrench that are relevant.

The wrenches applied at both gripping points during the transport task with both methods are presented Fig. 11 and Fig. 12.

Both of these methods allow preventing the operator from applying high torques as observed on Fig. 11.

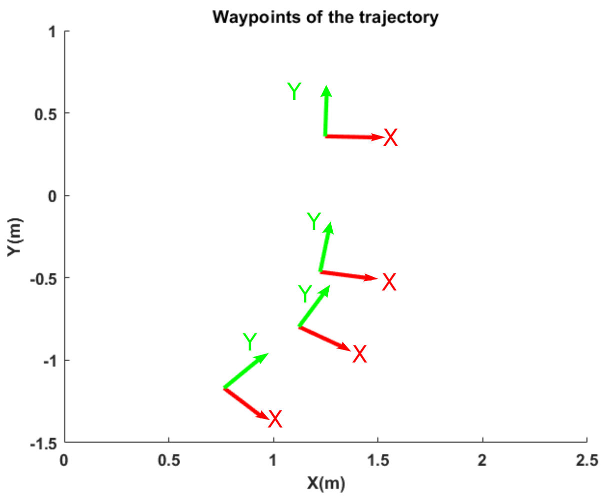

Fig. 10. Waypoints taught by demonstration with computed orientation along the path.

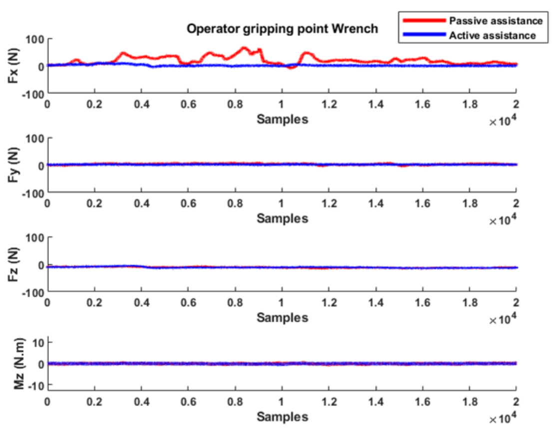

Fig. 11. Wrench at the operator gripping point.

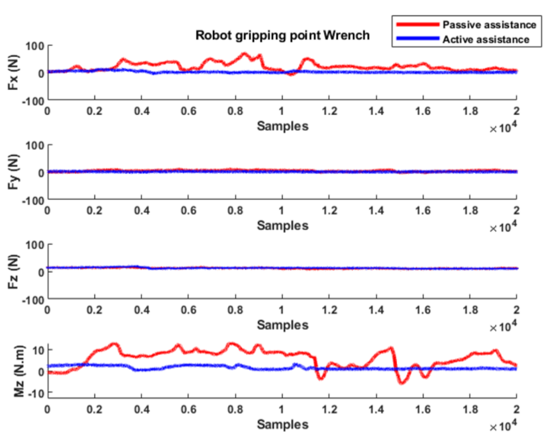

Fig. 12. Wrench at the robot gripping point.

As expected, we observe on Fig. 12 a significant torque (with a peak of 12.99N.m) at the robot gripping point with the passive assistance while a significantly weaker torque (with a peak of 3.26N.m namely almost 4 times weaker) is observed with the active assistance. The torque observed with the active assistance is mainly due to non-compensated friction and inertia of the fourth-joint of the robot.

Moreover, we observe a significant force on X-axis at both gripping points (with a peak of 69.64N) with the passive assistance while weaker force (with a peak of 11.54N namely almost 7 times weaker) is observed with the active assistance (Fig. 11 and 12). An explanation coming from the debriefing with the participant is the intuitiveness of the active assistance compared to the passive assistance. For the active assistance, the operator gives only the intention of displacement and the robot actively follows the path by itself. With the passive assistance, the operator has to apply forces in order to move the robot on the trajectory. However, the transport trajectory is not visible. Even if the operator has a rough idea of the trajectory, it is too difficult to apply precise direction of forces along the trajectory. Thus, the operator relies on the constraints to guide the movement along the trajectory by applying a force in the normal direction of the path (X-axis of the F/T sensor). That confirms that this well-known virtual guide feature [26] is not compatible with fragile object co-manipulation because it leads to apply significant stress on the object.

V. CONCLUSIONS

We presented a new controller design of robotic assistant for large and fragile object transportation. We proposed a design of an active follower assistant. The robot actively moves along the transport path according to its wrist's angle. This angle results from the operator action of transporting the object. The transport path is described by a virtual guide that allows joint human-robot transportation. We proposed to implement this virtual guide with the virtual mechanism principle [24]. We proposed to define this VM as a combination of MDSplines [11] to define the path trajectory and of a spherical joint in order to prevent robot from applying torques on the object and to use the wrist's angle to follow the operator along the path.

Our contribution is an extension of the proposed assistance in [11] and of the wrist's angle use introduced in [16] in order to transport a large and fragile object on any kind of trajectory and not only on straight lines. We presented a pilot experiment that highlights the efficiency of our approach in order to transport a large and fragile object by preventing torques application at the robot and the operator gripping points and more generally by minimizing stress on the object that is a necessary condition for a successfull large and fragile object transportation. The experimental confrontation also pointed out the intuitiveness of our active assistance compared to the passive assistance proposed in [25]. A user study has to be conducted to confirm this preliminar outcome with statistical significance. The F/T sensor at the operator gripping point has been used only for validation purpose on the experimental setup. However, no extra sensors are needed at the operator gripping point to co-transport a large and fragile object with our active follower assistant. This is demonstrated in the attached video, which shown the co-transport of different large and fragile objects with the active follower assistant. The next step is to perform an evaluation of the system with end-user's operators in the industrial conditions in order to then integrate the solution in manufacturing lines of the MERGING industrial partner.

In order to deal with a wrong definition of the transport trajectory or with unexpected events during the transport, we need to enhance our work with an important feature: to allow the operator to modify in real-time the transport trajectory. An extension of the work proposed in [25] is in progress. As a transport task is often followed by a precise positioning task, we are currently developing a complementary control law based on the same framework to precisely position large and fragile objects after executing a transport task.

ACKNOWLEDGMENT

This work was supported by the European Union's Horizon 2020 research and innovation programme under grant agreement No 869963 (MERGING project).

REFERENCES

[1] P. Garrec, "Screw and cable actuators (scs) and their applications to force feedback teleoperation, exoskeleton and anthropomorphic robotics," *Robotics 2010, Current and Future Challenges*, pp. 167–192, 2010.

[2] N. Hogan, "Impedance control - an approach to manipulation. i - theory. II - implementation. III - applications," *ASME Transactions Journal of Dynamic Systems and Measurement Control B*, vol. 107, pp. 1–24, 1985.

[3] F. Geffard, C. Andriot, A. Micaelli, and G. Morel, "On the use of a base force/torque sensor in teleoperation," in *IEEE International Conference on Robotics and Automation*, vol. 3, 2000, pp. 2677–2683.

[4] H. Arai, T. Takubo, Y. Hayashibara, and K. Tanie, "Human-robot cooperative manipulation using a virtual nonholonomic constraint," in *IEEE International Conference on Robotics and Automation*, vol. 4, 2000, pp. 4063–4069.

[5] W. Newman, "Stability and performance limits of interaction controllers," *Journal of Dynamic Systems, Measurement, and Control*, vol. 114, no. 4, pp. 563–570, Dec. 1992.

[6] T. Wojtara, M. Uchihara, H. Murayama, S. Shimoda, S. Sakai, H. Fujimoto, and H. Kimura, "Human-robot collaboration in precise positioning of a three-dimensional object," *Automatica*, vol. 45, no. 2, pp. 333–342, Feb. 2009.

[7] S. Yigit, C. Burghart, and H. Worn, "Co-operative carrying using pump-like constraints," in *IEEE/RSJ International Conference on Intelligent Robots and Systems*, vol. 4, 2006, pp. 3877–3882.

[8] T. Takubo, H. Arai, and K. Tanie, "Human-robot cooperative handling using virtual nonholonomic constraint in 3-D space," in *IEEE International Conference on Robotics and Automation*, vol. 3, 2001, pp. 2680–2685.

[9] M. Lawitzky, A. Mortl, and S. Hirche, "Load sharing in human-robot cooperative manipulation," in *IEEE International Symposium on Robot and Human Interactive Communication*, Sept. 2010, pp. 185–191.

[10] J. Dumora, F. Geffard, C. Bidard, N. A. Aspragathos, and P. Fraisse, "Robot assistance selection for large object manipulation with a human," in *IEEE International Conference on Systems, Man, and Cybernetics*, 2013, pp. 1828–1833.

[11] S. Sánchez Restrepo, G. Raiola, P. Chevalier, X. Lamy, and D. Sidobre, "Iterative virtual guides programming for human-robot comanipulation," in *IEEE International Conference on Advanced Intelligent Mechatronics (AIM)*, 2017, pp. 219–226.

[12] S. Calinon, P. Evrard, E. Gribovskaya, A. Billard, and A. Kheddar, "Learning collaborative manipulation tasks by demonstration using a haptic interface," in *International Conference on Advanced Robotics*, June 2009, pp. 1–6.

[13] J. Medina, T. Lorenz, D. Lee, and S. Hirche, "Disagreement-aware physical assistance through risk-sensitive optimal feedback control," in *IEEE/RSJ International Conference on Intelligent Robots and Systems*, Oct. 2012, pp. 3639–3645.

[14] A. Mortl, M. Lawitzky, A. Kucukyilmaz, M. Sezgin, C. Basdogan, and S. Hirche, "The role of roles: Physical cooperation between humans and robots," *The International Journal of Robotics Research*, Aug. 2012.

[15] N. Jarrasse, J. Paik, V. Pasqui, and G. Morel, "How can human motion prediction increase transparency?" in *IEEE International Conference on Robotics and Automation*, May 2008, pp. 2134–2139.

[16] Y. Hayashibara, T. Takubo, Y. Sonoda, H. Arai, and K. Tanie, "Assist system for carrying a long object with a human-analysis of a human cooperative behavior in the vertical direction," in *IEEE/RSJ International Conference on Intelligent Robots and Systems*, vol. 2, 1999, pp. 695–700.

[17] K. Kosuge, M. Sato, and N. Kazamura, "Mobile robot helper," in *IEEE International Conference on Robotics and Automation*, vol. 1, 2000, pp. 583–588.

[18] R. Ikeura, T. Moriguchi, and K. Mizutani, "Optimal variable impedance control for a robot and its application to lifting an object with a human," in *IEEE International Workshop on Robot and Human Interactive Communication*, 2002, pp. 500–505.

[19] C. Parker and E. Croft, "Design and personalization of a cooperative carrying robot controller," in *IEEE International Conference on Robotics and Automation*, May 2012, pp. 3916–3921.

[20] S. Eppinger and W. Seering, "On dynamic models of robot force control," in *IEEE International Conference on Robotics and Automation*, vol. 3, 1986, pp. 29–34.

[21] J. Colgate, "The control of dynamically interacting systems," Ph.D. dissertation, Massachusetts Institute of Technology, 1988.

[22] D. J. Agravante, A. Cherubini, A. Bussy, P. Gergondet, and A. Kheddar, "Collaborative human-humanoid carrying using vision and haptic sensing," in *IEEE International Conference on Robotics and Automation*, 2014, pp. 607–612.

[23] A. Bussy, A. Kheddar, A. Crosnier, and F. Keith, "Human-humanoid haptic joint object transportation case study," in *IEEE/RSJ International Conference on Intelligent Robots and Systems*, 2012, pp. 3633–3638.

[24] L. Joly and C. Andriot, "Imposing motion constraints to a force reflecting telerobot through real-time simulation of a virtual mechanism," in *IEEE International Conference on Robotics and Automation*, vol. 1, 1995, pp. 357–362.

[25] S. Sánchez Restrepo, G. Raiola, J. Guerry, E. D'Elia, X. Lamy, and D. Sidobre, "Toward an intuitive and iterative 6d virtual guide programming framework for assisted human–robot comanipulation," *Robotica*, vol. 38, no. 10, pp. 1778—-1806, 2020.

[26] E. Boy, E. Burdet, C. Teo, and J. Colgate, "Motion guidance experiments with scooter cobot," in *11th Symposium on Haptic Interfaces for Virtual Environment and Teleoperator Systems*, Mar. 2003, pp. 63 – 69.